Nuclear Inst. and Methods in Physics Research B 479 (2020) 187–193

Contents lists available at ScienceDirect

Nuclear Inst. and Methods in Physics Research B

journal homepage: www.elsevier.com/locate/nimb

Foundations and trends of high resolution energy dispersive PIXE (HiRED-PIXE)

M.A. Reis[a,b,*], A. Carvalho[b], A. Taborda[a,b], P.C. Chaves[a,b], P. Conceição[c], P. Madureira[c,d]

[a] Centro de Ciências e Tecnologias Nucleares (C²TN), Instituto Superior Técnico, Universidade de Lisboa, Campus Tecnológico e Nuclear, EN10 km 139.7 2695-066 Bobadela, Portugal
[b] Ad Fisicateca, R. Pedro Vaz Henriques, 7, 2560-256 Torres Vedras, Portugal
[c] Estrutura de Missão para a Extensão da Plataforma Continental, Rua Costa Pinto nº 165, 2770-047 Paço de Arcos, Portugal
[d] Dept. Geo, Univ. Évora Colégio Luis António Verney Rua Romão Ramalho 59, 7000-671 Évora, Portugal

ARTICLE INFO

Keywords:
Line-shifts
Fe–Mn crusts
HiRED-PIXE
Unilateral NMR
Speciation
Porous materials

ABSTRACT

High Resolution Particle Induced X-ray Emission, for short HR-PIXE, dates back to 1977 and is, therefore, nearly as old as standard PIXE itself. Until roughly ten years ago, High Resolution PIXE (HR-PIXE) work used only wavelength dispersive spectrometers (WDS). The installation, in 2008, of an X-ray Microcalorimeter Spectrometer, XMS at CTN (ITN at the time) 3MV tandetron, altered this situation and, as can be recognised today, will lead to major changes in PIXE, and open up many possibilities that have been hindered so far. In this work, motives, developments, important breakthrough results obtained until now, and a case study displaying speciation data and complementary information from nuclear magnetic relaxometry, are presented and discussed, showing the full quantitative potential of High Resolution Energy Dispersion PIXE (HiRED-PIXE), in particularly the opening up of the possibility to establish fast and efficient methods for quantitative elemental speciation in unknown samples.

1. Introduction

High resolution PIXE emerged promptly after the 1970s PIXE foundational papers [1,2], using wavelength dispersive spectrometers [3]. Since then, this type of work was never abandoned, although it remained for a long time limited to a few laboratories around the world, and oriented mostly towards fundamental problems. Comprehensive reviews of the work of various laboratories in this context were published by Terasawa, Török and Petukhov in the 1990s [4–6]. After the turn of the century, using WDS high resolution PIXE for applications became more frequent. The works of Maeda [7], Hasegawa [8], Kavčič [9], Tada [10] and Woo [11] are good examples of this.

In the beginning of the 21st century, Transition Edge Sensor (TES) based X-ray Microcalorimeter Spectrometers (XMS) emerged, leading to works as that of Li on the analysis of airborne particles using a TES high resolution energy dispersive spectrometer (EDS) coupled to a Scanning Electron Microscopy (an XMS-SEM in fact), published in 2009 [12], as well as to the installation of the first XMS based PIXE system at Instituto Tecnológico e Nuclear, in 2008 [13,14] (presently C²TN-IST/ULisboa), and more recently to the installation of a second generation XMS-PIXE system at the Universty of Jyväskylä [15].

After more than ten years passed over the installation of the XMS-PIXE system at C²TN, we are now in a position to state that a new field of High Resolution Energy Dispersive PIXE (HiRED-PIXE) has been launched. New software tools have been developed [16] (although not yet fully operational for use by non-specialists) and it seems the appropriate time to present some perspectives for the future use and capabilities of HiRED-PIXE technique, even if based on preliminary data.

All the work done on WDS-PIXE since the 1970s' decade is a solid background for HiRED-PIXE. Still, the fact that the energy region covered in a single HiRED-PIXE spectrum (tens of keV) is much broader than in a single WDS-PIXE spectrum (sometimes only a tenth of a keV), allows to address many problems using HiRED-PIXE, which would be difficult or even impossible to study properly using WDS-PIXE.

Extending high resolution over a wide energy region in a single spectrum, provides more that just a quantitative step relative to WDS-PIXE. Once resolution is improved relative to the standard solid-state detectors, as happens in WDS-PIXE, fine details in the ionization and de-ionization processes become observable. In HiRED-PIXE this remains true even when details are far apart in energy, which opens up the possibility of studying many processes hardly at reach of WDS-PIXE work.

One situation where WDS-PIXE and HiRED-PIXE are similar is

* Corresponding author at: Centro de Ciências e Tecnologias Nucleares (C²TN), Instituto Superior Técnico, Universidade de Lisboa, Campus Tecnológico e Nuclear, EN10 km 139.7 2695-066 Bobadela, Portugal.
E-mail address: mareis@ctn.tecnico.ulisboa.pt (M.A. Reis).

https://doi.org/10.1016/j.nimb.2020.06.017
Received 20 December 2019; Received in revised form 3 June 2020; Accepted 7 June 2020
0168-583X/

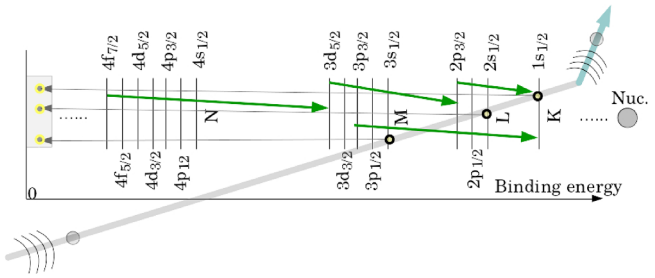

Fig. 1. Idealised model of PIXE. It is important to realise that heavy charged particle ionization processes may frequently lead to multiple ionization states of the complex inner-shell atomic structure, since cross sections for ionization of less energetic shells are significantly larger than those for more inner-shells. Besides, even in face of a simple single ionization, the final state of the ion electron cloud presents a complex fine structure due to the coupling of the vacancy angular momentum to other non-paired angular momentum existing in the electron cloud (outer or valence shells) or in the vicinity of the created ion.

multiple ionization [17] studies, because the satellite transitions involved have energies close to that of the parent line.

Charged particle ionization is nevertheless a process more complex than photoionization by X-rays, as illustrated in Fig. 1. Cross sections for ionization of outer shells by particles are larger than those for more inner shells, which makes multiple ionization conditions more frequent in PIXE than when X-ray ionization is faced. Although optimized WDS-PIXE systems [9] do still have better resolution than HiRED-PIXE systems[18], which can be an advantage in some cases, HiRED-PIXE systems can observe multiple ionization transitions for more than a single transition and for more than a single element, in a single spectrum, which may also be an advantage. Which system is better depends on the problem being studied, therefore HiRED systems are not a replacement for WDS systems, but rather a new and complementary tool.

Beyond multiple ionization, the added complexity of charged particle ionization, is present even in the simpler case of a single ionization. In this case the final state of the ion electron cloud presents a complex fine structure due to the coupling of the angular momentum of the vacancy (in fact the result of the response of all remaining electrons to the lack of the removed one) to other non-paired angular momenta in the vicinity, including non-paired valence electrons of the ion itself. These couplings can generate high angular momentum ionization states that lead to satellite transitions that are present relatively far apart from the parent, as was recently pointed out [14,19]. Because these transitions originate in high angular momentum ionization states, they will be favoured by charged particle ionization, and not by X-ray ionization. These strange satellite transition are still not much explored, one of the reasons being that although they are accessible to HiRED-PIXE, their study using WDS-PIXE is at least very difficult, if not impossible, given the large energy separation between the satellite energy and its parent transition.

Furthermore, as shown by Reis et al. in 2005 [20], the number of X-ray lines per 100 eV, is of the order of 25 for energies below 5 keV, of the order of 10 for energies between 5 and 20 keV, and below 3 for energies above 20 keV. Therefore, once a relative resolution of 1% or

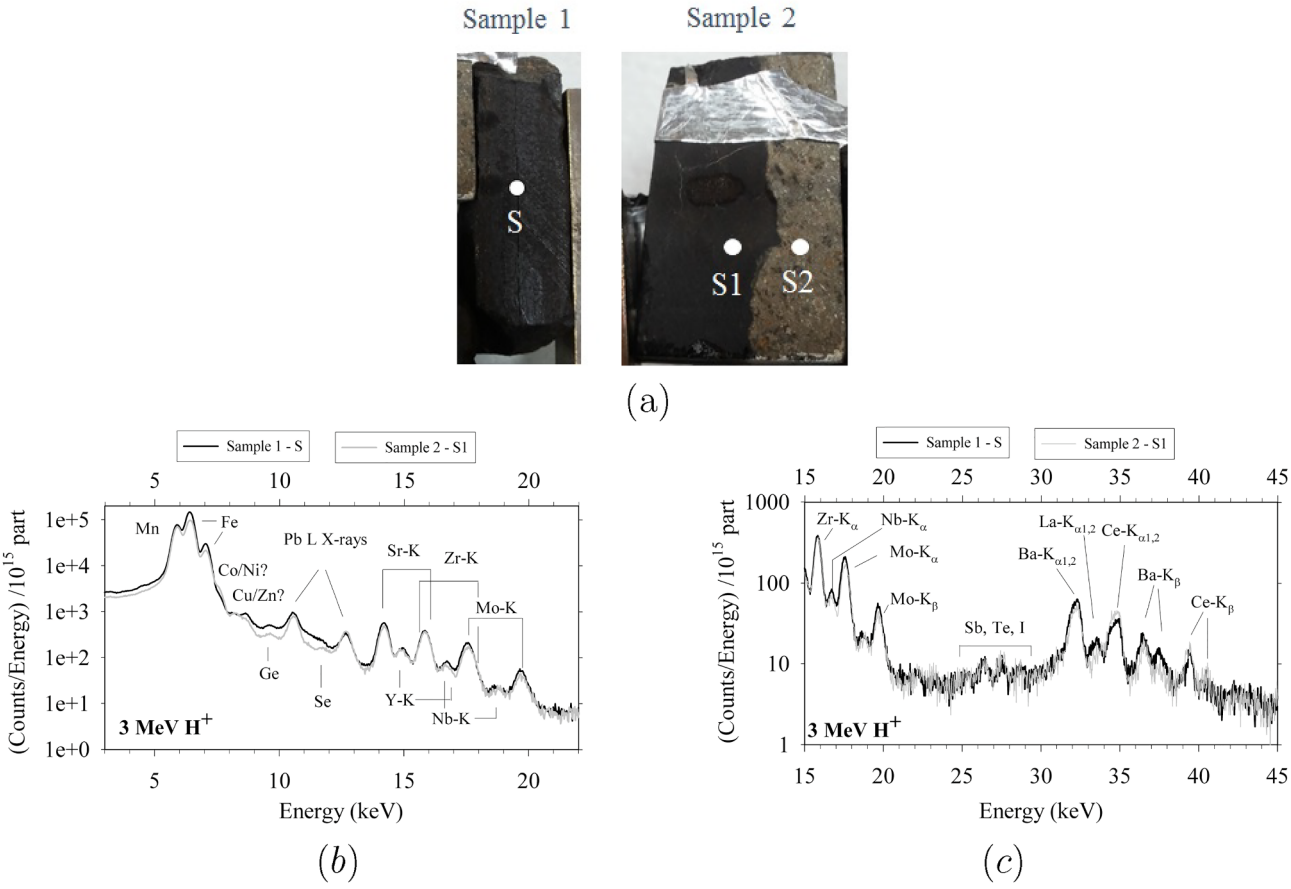

Fig. 2. (a) Photographs of the irradiated Portuguese continental shelf samples. Sample 1 was irradiated at a single spot, while sample 2 was irradiated at two different spots, S1-Fe–Mn crusts material and S2-Aluminium Silicate substrate. The circles indicate the positions of irradiation spots having 3 mm diameter. (b,c) CdTe spectra of sample 1 (spot S) and sample 2 (spot S1) when irradiated by a 3.0 MeV H^+ beam using similar collecting charge. Black line correspond to sample 1 data and gray line to the data of spot S1 from sample 2. (b) Spectra overlap for an energy range covering K lines from Mn to the K lines of Mo. (c) energy region from 15 to 45 keV covering the energy region of K lines of rare earth elements (REE).

better is attained, lines are separable over the whole X-ray spectra, even in the most dense region below 5 keV, and details become observable. The present state-of-the-art XMS may be tuned to achieve energy resolution levels of 1.5 eV at Mn 5.89 keV, well below the 1% level, thus assuring a complete separation of lines. Still, as mentioned above and shown in a case study below, the fact that HiRED-PIXE spectra cover wide energy regions, provides capabilities that far exceed a mere separation of X-ray lines.

In this work, the composition of two Fe–Mn crusts samples, displayed in the photograph of Fig. 2(a), was studied using proton and heavy ions PIXE and their porous structure was accessed by nuclear magnetic relaxometry, a commonly used methodology to study rapidly, non-invasively and non-destructively porous materials [21,22].

In the case of heavy ions PIXE, line energy shifts emerging from the use of 6 MeV O^{3+} beams were determined, and compared to calculations by Verma [17]. In the case of proton PIXE, HiRED-PIXE results provide speciation data by comparison to spectra of known Fe compounds. Finally, nuclear magnetic relaxometry data provides an insight regarding the porous nature of each of the samples.

2. Materials and methods

HiRED-PIXE experiments were carried out using the High Resolution High X-ray Energy (HRHE)-PIXE setup [23] endstation of the CTN 3.0 MV Tandetron. X-rays were collected using both an Amptek Peltier Cooled $3 \times 3 \times 1$ mm^3 CdTe detector having a 250 μm Beryllium window, placed at about 25 mm from target and at 145° relative to the beam direction, and the TES high resolution EDS Vericold Tech. GmbH Polaris XMS referred here as the C^{2}TN-XMS, set at 90° to beam direction. More details about the HRHE-PIXE system can be found in references [23,14].

Two Fe–Mn crusts samples from the Portuguese continental shelf were studied using 1.0 MeV and 3.0 MeV H^+ and 6.0 MeV O^{3+} ion beams. 1.0 MeV H^+ beam or heavy ion beams must be used when low energies are to be studied using the C^{2}TN-XMS to avoid damaging the TES device due to particles scattered towards the detector. In the case of heavy ions, 6.0 MeV O^{3+} beams are the best quality heavy ion beam obtainable at the CTN Tandetron reaching the HRHE-PIXE chamber [24,25].

In addition to the Fe–Mn crusts samples, a pyrite sample and an ultrapure Fe_2O_3 sample, were also irradiated for reference and comparison to the Fe–Mn crusts samples spectra.

H^+ ion beams were collimated to an ellipse like shape in order to provide spots on the target that were circles having 3 mm in diameter. O^{3+} beams were not collimated and the beam spots were roughly elliptical having 1 mm and 3 mm as minor and major axis size, respectively. An electron gun was used to avoid charging up of the targets.

The beam incidence angle was 65° relative to the target normal, and

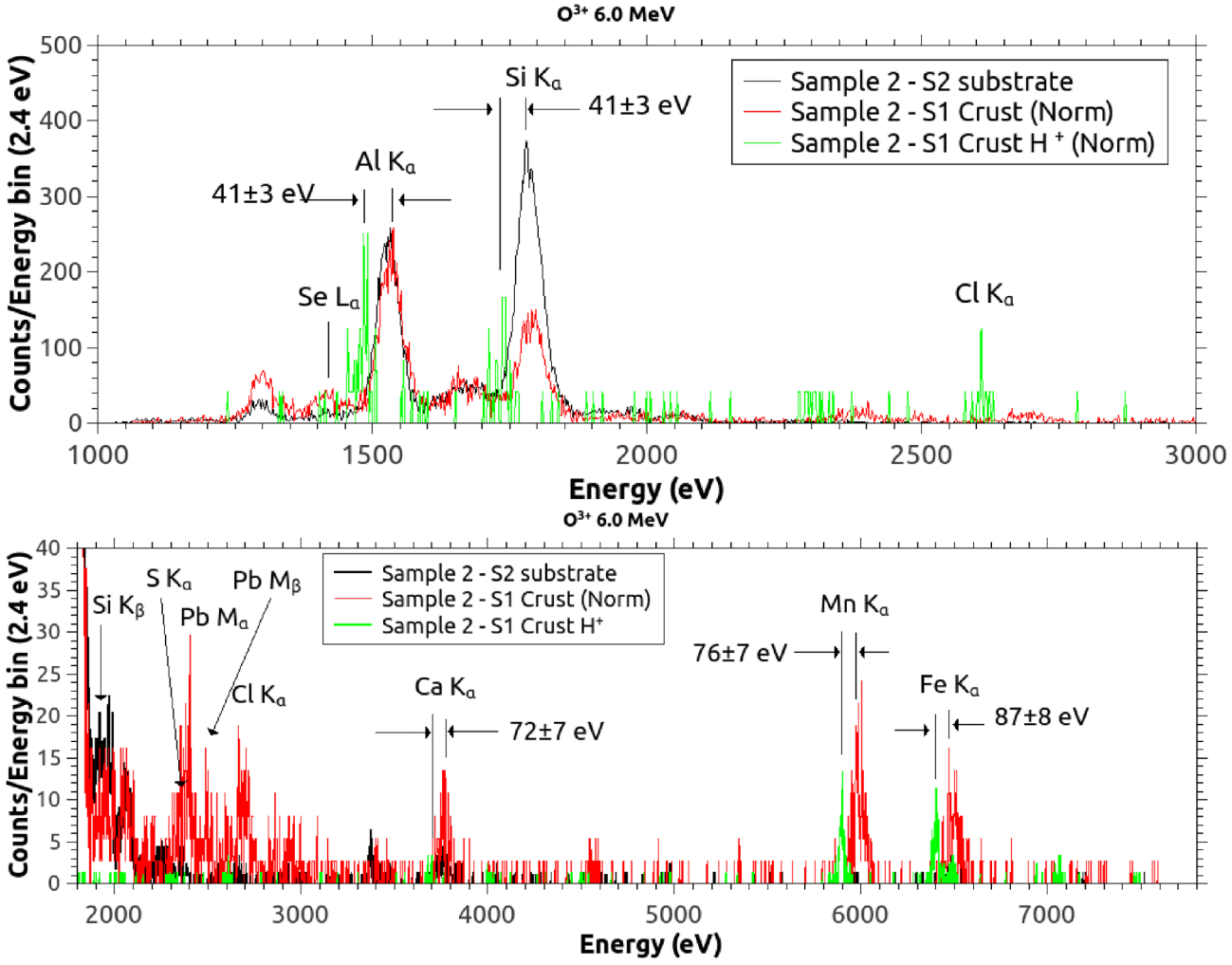

Fig. 3. XMS spectra of the substrate and the crusts material of sample 2 irradiated using 6 MeV O^{3+} beams, and the sample 2 crusts material irradiated using 1.0 MeV H^+ beam. (Norm) indicates normalization to the height of the Al K_α. Line shifts can be directly identified. The very low statistics of the spectrum obtained during H^+ beam irradiation, does not hinder its use because of the very high resolution of the XMS system. Se L-lines are identifiable in the top graph, between Al and Mg K lines. The presence of S, Cl, Ca and Pb in the crusts, essentially absent in the substrate, is also seen on the bottom spectra.

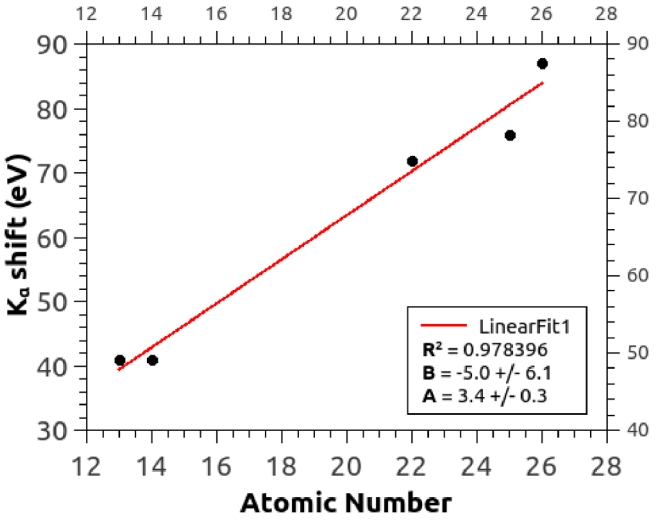

Fig. 4. Line shifts determined experimentally fit along a regression line which values can be compared to theoretical calculations present in literature (eg: Verma et al. [17]).

the CdTe and the XMS detection angles were of 10° and 25°, respectively. During 3.0 MeV H^+ beam irradiations, an 1 mm thick Al funny filter (with a hole 1 mm in diameter) located on top of a connic-shaped 2.5 mm thick polycarbonate placed on a soft PVC support was used on front of the CdTe detector, to reduce low-energy X-rays intensity and smooth the efficiency curve by favouring higher energies efficiency. On these conditions, at 90°, in front of the XMS, a BN 200 μm thick foil was used to prevent scattered protons from reaching the detectors absorber, damaging the TES device. No filters were used during 1.0 MeV H^+ and 6.0 MeV O^{3+} irradiations.

Apart from a vertical cut and the polishing of the cut surface no additional operations were performed prior to mounting the sample on the sample-holders and cleaning its surface (with a clean paper impregnated with ethanol) before introducing the sample-holder in the analytical chamber. A single spot was irradiated in sample 1 and two spots were irradiated in sample 2, one in the Fe–Mn deposit (S1) and other in the substrate region (S2) (see Fig. 2 (a)). In this way a first comparison of the two deposits, and of these and the substrate of sample 2, was possible.

Samples were also studied by Nuclear Magnetic Resonance relaxometry using the Magritek PM2.5 NMR MOUSE single side (or unilateral) sensor system from Ad Fisicateca. For this, after ion beam irradiations, the samples were deep in destilled water for more than 24 h prior to measurement. 1H-NMR relaxometry studies were performed, after removing the sample from the water bath and placing it on top of a glass base.

The relaxation times T_1 and T_2 were measured in a parallelepiped slice with 100 μm thickness located 4 mm away from the surface to the inside of the sample. The longitudinal relaxation time, T_1, was measured using a standard saturation recovery pulse sequence with a pulse length of 6 μs. The recorded signal was taken as the average of 4 repetitions made using a repetition time of 1.2 s. The transverse relaxation time T_2 was measured using a Carr-Purcell-Meiboom-Gill pulse sequence [26] to diminish the effect of diffusion on the measured value of T_2. Echo trains of 300 echos were used and the recorded values were taken as the average of 32 or 64 repetitions made using a repetition time of 1.5 s. The number of repetitions was selected as necessary to assure a small enough uncertainty in the measurement.

3. Results and discussion

Fig. 2(b) displays the CdTe detector spectra for sample 1 and spot S1 of sample 2, for the energy region covering from 3 to 22 keV, where the K lines from elements having atomic number, Z, between $25 \leqslant Z \leqslant 42$ are present. Overlaps are observable in the Co/Ni/Cu/Zn energy region and doubts emerge regarding the presence of each of these elements. Fig. 2(c) shows the corresponding spectra for the energy region from 15 to 45 keV, where the K X-rays of Zr and rare earth elements, REE, are present.

A K_α line of La is identifiable in sample 1, without a similar correspondence being observable in sample 2. Still, apart from the differences around Pb L lines and for the La and Ce contributions, spectra seem quite similar.

A full analysis of such complex spectra requires a detailed fitting but, prior to that, additional information can be obtained by studying the samples using different beams and High Resolution Heavy Ion PIXE spectra.

In Fig. 3, the XMS spectra of the sample 2 substrate and crusts materials irradiated by 6.0 MeV O^{3+} beams are presented, together with the reference spectrum of the crusts spot irradiated by an 1.0 MeV H^+ beam. Difficulties in collecting the spectrum generated by the H^+ beam in the same amplifying conditions as those corresponding to the 6.0 MeV O^{3+} beams, made that only very few counts could be obtained in the H^+ irradiation spectrum. Still, the characteristics of the XMS system allow us to overcome the difficulties and use the collected data for determination of the energy calibration of the XMS, which has been preserved operationally in the spectra corresponding to the 6.0 MeV O^{3+} beams irradiations (check reference [27] for details). In these conditions, the experimental line shifts of the K lines of Al, Si, Ti, Mn and Fe could be determined, and a linear trend could be fitted to the line shift increase as function of the atomic number. The regression line is shown in Fig. 4. Taking into account the calculations from Verma [17] and the observed line shifts, one can conclude that these low and medium Z elements present high ionization states with two spectator

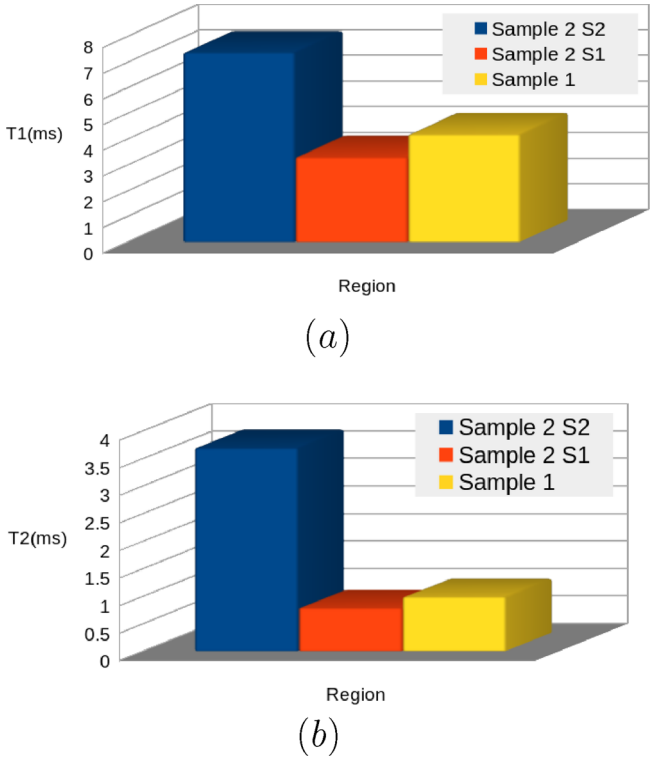

Fig. 5. Longitudinal relaxation time (T_1) (a) and effective transverse relaxation time (T_2) (b), measured in sample 1 and two different regions of sample 2, the Fe–Mn crusts (spot S1) and the Aluminium Silicate substrate (spot S2). Measurements were made using Ad Fisicateca PM2.5 MOUSE single sided NMR. Values are consistent with literature values for Fe bearing minerals coated sands [29,30].

vacancies in the L shell ($K\alpha L^2$) as the most probable situation in face of 6.0 MeV O^{3+} beams irradiations.

These spectra also allow us to observe the differences between crusts material and the substrate of sample 2. Spectra are normalised to Al K_α line. Overall, in the crusts material the enhanced presence of Mg and Se can be observed, as well as the presence of S, Cl, Ca, Mn, Fe and Pb, which are essentially absent from the substrate.

Differences between the substrate and the crusts material were also studied by unilateral nuclear magnetic relaxometry (NMR), to compare the level of porosity of crusts and substrate.

In fact, it is known and was also recently shown by Ouahabi et al. [28], that significant quantitative differences may emerge in PIXE results due to differences in the porous and grain structure of the samples. This must therefore be taken into account when studying pristine materials.

In Fig. 5 results from NMR studies of crusts and substrate materials are presented. Differences in longitudinal and transverse relaxation rates between substrate and crusts components, clearly point to significant differences between the porous structure of these materials, and point to the need to properly account for the porous structure of the sample in precise quantitative work, to overcome the problems shown by Ouahabi et al. [28].

In Fig. 6 spectra of sample 1 and two reference samples, namely a pyrite sample and a 99.995% ultrapure Fe_2O_3 sample, collected using the C^2TN-XMS during irradiations with 3.0 MeV H^+ beams, are shown.

In one of the graphs, the pyrite and the Fe_2O_3 spectra are presented normalized to the height of the Fe K_α peak. It can be seen that the resolution of the XMS system is enough to observe the differences in the K_β group as emitted by the Fe(II) from the pyrite and by the Fe(III) from the Fe_2O_3 sample.

These differences allow the speciation of the Fe in sample 1. For that, the ratio of the heights of the K_β group was determined in the K_α normalised spectra of the pyrite and the Fe_2O_3 samples. Afterwards, properly normalised versions of each of these spectra were added so that the Fe K_β of the sum would reproduce the Fe K_β of the spectrum of sample 1. This done, the ratio of heights was determined and compared to the ratio in the 1 to 1 normalization. Taken into account these ratios, a speciation of 54% Fe(II) and 46% Fe(III) was determined for sample 1.

In spite of the fact that this is a first approximation calculation, the result demonstrates that even using a first generation XMS system, it is possible to obtain elemental speciation data, in unknown samples, by using the shape of the K_β group, applying what is known from WDS work [31] to wide energy window HiRED spectra.

In Fig. 6 bottom graph it is possible to observe the presence of Ca, Ti, radiative Auger emissions (RAE) from Mn, RAE from Fe (a structure similar to the RAE from Mn, identified in the pyrite and Fe_2O_3 sum spectrum that contributes to a low energy tail shape on the Mn $K\alpha$ line), Co, Ni and very small contributions (in the form of 10 counts height peaks) of Ba and Ce (L lines), which K lines presence was identified in the CdTe detector spectrum collected simultaneously (see Fig. 2).

In the analysis of these results it is also important to take into account that the limited statistics presented in some of these XMS spectra are mostly due to the age and pioneer nature of the C^2TN-XMS system [13,32], and not to problems intrinsic to XMS systems, as can be seen

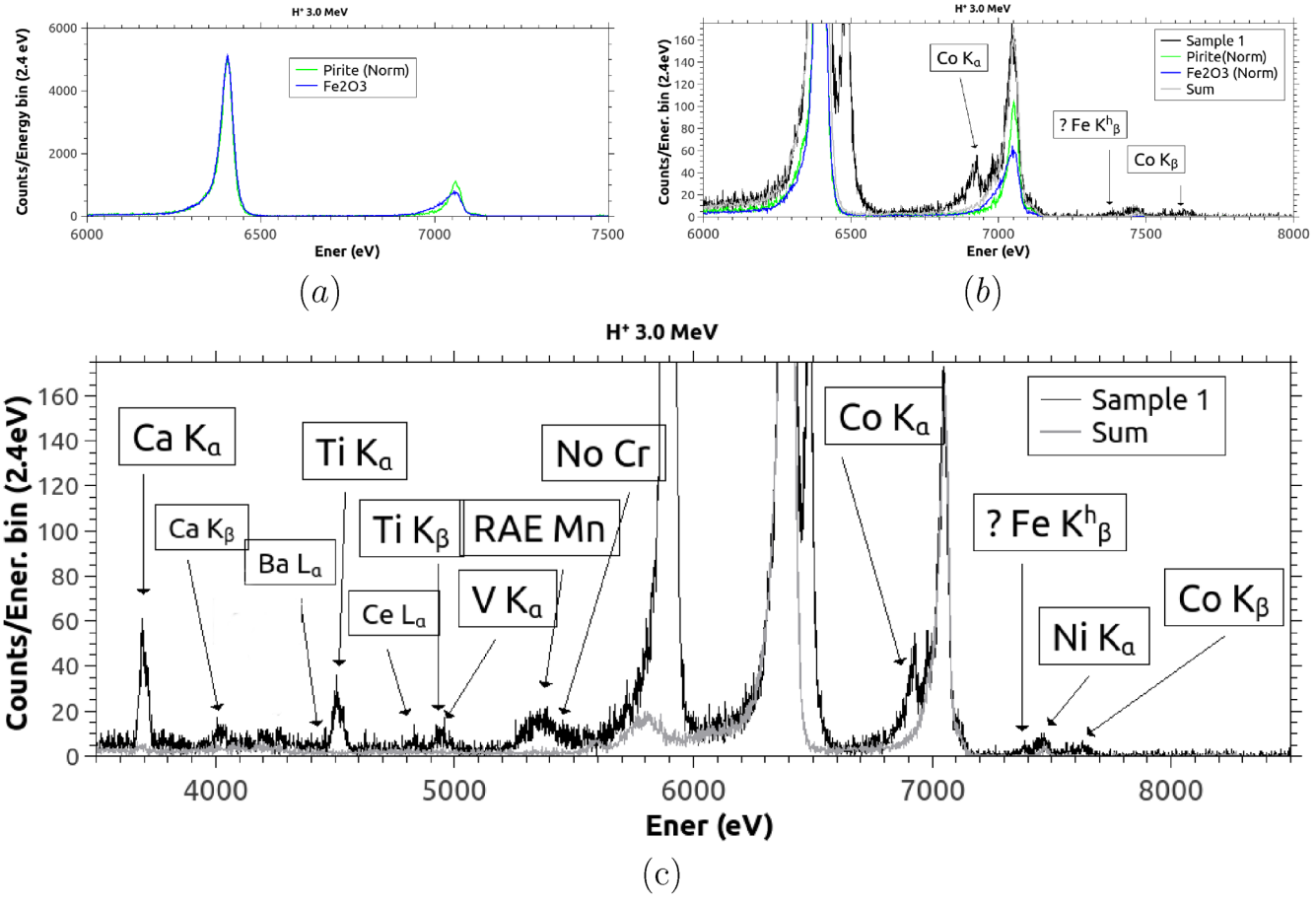

Fig. 6. XMS spectra of sample 1, a pyrite sample and a 99.9995% ultrapure sample of Fe_2O_3 irradiated using 3.0 MeV H^+ beams. (a) Differences between the Fe(III) K_β in the spectrum of the Fe_2O_3 sample, and the Fe(II) K_β in the spectrum of the pyrite sample. (b) Using a sum of normalised contributions of the two types of Fe K_β spectra, it was possible to reproduce the shape of the Fe K_β in the spectrum of sample 1. Comparing the ratio of the heights of the partial K_β contributions in the sum, to their ratio on the Fe K_α normalised condition (in (a)) a speciation ratio of 54% Fe(II) to 46% Fe(III) was determined for the Fe in sample 1. (c) Minor contributions detectable in the XMS spectrum, some of them having even quite low statistics.

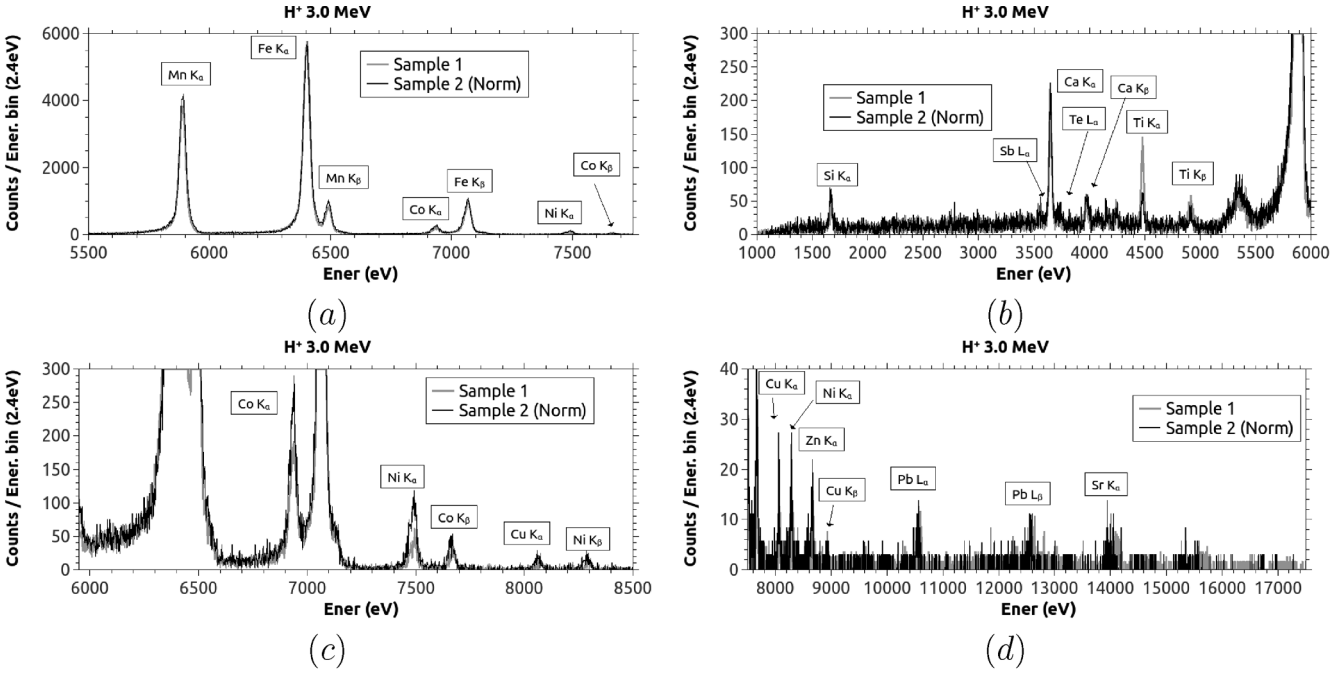

Fig. 7. Details on the comparison of the HiRED-PIXE spectra of the crusts material of the two samples studied, normalized to the Fe K_α peak. (a) Major elements contribution. It can be seen that the Mn K_α peak in the spectrum of sample 2 is slightly higher than in the spectrum of sample 1. (b) Low energy region. In spite of the use of a 200 μm BN foil in front of the XMS the Si K_α peak is still observed. The presence of a larger peak of Ti K_α in the spectrum of sample 1 may explain the smaller Mn K_α peak observed in the same spectrum. The presence of Sb and Te, observed in the CdTe spectrum in Fig. 2, is confirmed. (c) Minor elements. The XMS resolution allows the complete separation of the full transition metals sequence: Mn, Fe, Co, Ni, Cu and Zn. (d) Trace elements such as Pb and Sr are still observable. Taking into account the values of ionization cross-sections, it can be concluded without further studies that these elements are present in the samples in concentration levels similar to those of as Cu, Ni and Zn.

on results from more recent XMS systems (eg: see Palosaari et al. [15]).

Fig. 7 presents results comparing spectra from sample 1 and spot 2 of sample 2, where the spectrum from sample 2 was normalised to the spectrum from sample 1 at the Fe K_α peak.

Spectra are very similar, as was the case with the CdTe spectra presented in Fig. 2. The Mn peak is slightly lower in sample 1, while the Co and Ni contributions (Fig. 2(c)) are 20% and 50% lower in sample 1, respectively. The fact that Ti presents a concentration that is apparently a factor of 3 higher in sample 1 than in sample 2, as can be seen from graph (b) in Fig. 7, may enhance self absorption of Mn in sample 2 matrix. Still it is not enough to justify the differences in Co and Ni.

Furthermore, the differences seen in NMR relaxometry data, when studied in detail, show that the effective transversal relaxation in both samples presents a bi-exponential nature where the partial T_2 values are identical in both samples, but the weights of each one are different from one sample to the other. A result that points to a different nature of the surfaces and surface/volume ratios in the two MnFe crusts materials.

In Fig. 7(b), the presence of Sb and Te on both sides of the Ca K_α peak also confirms their presence raised during the study of the CdTe spectrum. The presence of Cu, Zn, Sr and Pb is also observed in these high resolution spectra.

4. Conclusions

In this work we presented a preliminary and exploratory first study of two geological samples from the Portuguese continental shelf. HiRED-PIXE spectra were obtained using the C^2TN HRHE-PIXE setup and the combined use of the CdTe and XMS detectors. Spectra data were collected from 1.5 keV to 120 keV. O^{3+} HiRED-PIXE data made possible the determination of K line shifts from Mg to Fe. H^+ HiRED-PIXE spectra provided speciation of Fe. A detailed analysis based on NMR data and details of the HiRED-PIXE data showed that both samples, which seemed *a priori* quite similar, were in fact originated in samples having either meaningful differences in concentrations of Ti, Co and Ni, or in their porous structure, or in both. The 3 MeV H^+ CdTe PIXE spectra showed the presence of Ba, La and Ce using K lines, which L lines could hardly be observed in HiRED-PIXE spectra due to its very low intensity and the low statistics in these spectra.

Still, the identification of the presence of La and Ce confirms the possibility of using the PIXE technique, in this way, to determine REE in geological samples, a result very difficult to achieve using standard PIXE due to the overlap of L lines of these elements with the K lines of major elements.

HiRED-PIXE allowed to simultaneously carry out fundamental and applied work and to obtain speciation ratios for Fe(II) and Fe(III).

In this work, very simple qualitative approaches were taken. Detailed quantitative work can be carried out in HiRED-PIXE using the DT2 code [16], still, care must be taken to assure that the porous nature of the samples is taken in proper account. A possible approach to this is the use of NMR studies and HiRED-PIXE data in an holistic analysis, to unravel the contributions from different surface composition and different pore structures [21,29,30], increasing the precision of HiRED-PIXE data quantification, which, as shown, includes speciation of, at least, major elements in an *a priori* unknown sample. The access to present day state-of-the-art spectrometers will assure the robustness of results.

Trends in HiRED-PIXE thus lead to quantitative speciation and to the use of PIXE in new frameworks where its use was hindered until now. Resolving the classical Co/Ni/Fe/Zn overlap and the determination of REE in manganeses and iron minerals, being a commercially very important breakthrough, point clearly new ways to go, while holistic work coupling HiRED-PIXE to other IBA methods, and also to NMR data, as shown here, clearly display a very wide scope and new future to the field.

Declaration of Competing Interest

The authors declare that they have no known competing financial interests or personal relationships that could have appeared to influence the work reported in this paper.

Acknowledgements

This work was made possible by the partial financial support of the IAEA through Research contract No. 18357 in the frame of the Coordinated Research Project F11019 on Development of Molecular Concentration Mapping Techniques using MeV Focused Ion Beams and of the Portuguese Foundation for Science and Technology, FCT, fellowship SFRH/BPD/76733/2011 and UID/Multi/04349/2013 project.

References

[1] T.B. Johanson, A. Akselsson, S.A.E. Johansson, X-ray analysis: elemental trace analysis at the 10^{-12}g level, Nucl. Instrum. Methods 84 (1970) 141–143.
[2] S.A.E. Johansson, T.B. Johansson, Analytical applications of particle induced X-ray emission, Nucl. Instrum. Methods Phys. Res. 137 (1976) 473–516.
[3] R.L. Watson, A.K. Leeper, B.I. Sonobe, Applications of wavelength-dispersive spectrometry in particle-induced X-ray emission analysis, Nucl. Instrum. Methods 142 (1977) 311–316.
[4] M. Terasawa, I. Török, V.P. Petukhov, High-resolution PIXE instrumentation survey. Part I, Nucl. Instrum. Methods Phys. Res. B 75 (1993) 105–108.
[5] V.P. Petukhov, M. Terasawa, I. Török, High-resolution PIXE instrumentation survey. Part II, Nucl. Instrum. Methods Phys. Res. B 150 (1999) 103–108.
[6] V.P. Petukhov, I. Török, M. Terasawa, High-resolution PIXE instrumentation survey. Part III, Nucl. Instrum. Methods Phys. Res. B 109 (110) (1996) 105–108.
[7] K. Maeda, K. Hasegawa, M. Maeda, K. Ogiwara, H. Hamanaka, Rapid chemical state analysis in air by highly sensitive high-resolution PIXE using a v. Hamos crystal spectrometer, X-ray Spectrom. 34 (2005) 389–392.
[8] J. Hasegawa, T. Tada, Y. Oguri, M. Hayashi, T. Toriyama, T. Kawabata, K. Masai, Development of a high-efficiency high-resolution particle-induced X-ray emission system for chemical state analysis of environmental samples, Rev. Sci. Instrum. 78 (2007) 073105.
[9] M. Kavcic, Improved detection limits in PIXE analysis employing wavelength dispersive Xray spectroscopy, Nucl. Instrum. Methods Phys. Res. B 268 (2010) 3438–3442.
[10] T. Tada, H. Fukuda, J. Hasegawa, Y. Oguri, Application of a wavelength-dispersive particle-induced x-ray emission system to chemical speciation of phosphorus and sulfur in lake sediment samples, Spectrochim. Acta Part B 65 (2010) 46–50.
[11] H.J. Woo, H.W. Choi, G.D. Kim, J.K. Kim, Control of the chemical state change of sulfur in solid compound targets during high resolution pixel measurements, J. Korean Phys. Soc. 61 (2) (2012) 243–247.
[12] Q. Li, R. Suzuki, Y. Ono, I. Nakai, K. Tanaka, S. Nakayama, H. Takahashi, High-resolution microanalysis of suspended particulate matter using a transition edge sensor microcalorimeter X-ray spectrometer, X-ray Spectrom. 38 (2009) 369–375.
[13] M.A. Reis, L.C. Alves, N.P. Barradas, P.C. Chaves, B. Nunes, A. Taborda, K.P. Surendran, A. Wu, P.M. Vilarinho, E. Alves, High Resolution and Differential PIXE combined with RBS, EBS and AFM analysis of magnesium titanate ($MgTiO_3$) multilayer structures, Nucl. Instrum. Methods Phys. Res. B 268 (2010) 1980–1985.
[14] M.A. Reis, P.C. Chaves, A. Taborda, Review and perspectives on energy dispersive high resolution PIXE and RYIED, Appl. Spectrosc. Rev. 52 (3) (2017) 231–248.
[15] M.R.J. Palosaari, K.M. Kinnunen, J. Julin, M. Laitinen, M. Napari, T. Sajavaara, W.B. Doriese, J. Fowler, C. Reintsema, D. Swetz, D. Schmidt, J. Ullom, I.J. Maasilta, Transition-edge sensors for particle induced X-ray emission measurements, J. Low Temp. Phys. 176 (2014) 285–290.
[16] M.A. Reis, P.C. Chaves, A. Taborda, J.P. Marques, N.P. Barradas, Fixed and free line ratio DT2 PIXE fitting and simulation package, Nucl. Instrum. Methods Phys. Res. B 318 (2014) 65–69.
[17] H.R. Verma, Study of radiative Auger emission, satellites and hypersatellites in photon-induced X-ray spectra of some elements in the range $20 \leq Z \leq 32$, J. Phys. B 33 (2000) 3407–3415.
[18] M.A. Reis, P.C. Chaves, A. Taborda, Radiative Auger satellites observed by microcalorimeter-based energy dispersive high-resolution PIXE, X-ray Spectrom. 40 (2011) 141–146.
[19] Ana Taborda. Ionizaçãiao de níveis internos em estruturas moleculares complexas e nanopartículas. PhD thesis, Faculdade de Ciências da Universidade de Lisboa, 2013.
[20] M.A. Reis, P.C. Chaves, J.C. Soares, Particle induced X-ray emission – relative yield ion energy dependence, an IBA chemical speciation method, Nucl. Instrum. Methods Phys. Res. B 229 (2005) 413–424.
[21] J.P. Korb, Nuclear magnetic relaxation of liquids in porous media, New J. Phys. 13 (2011) 26 035016.
[22] R.L. Kleinberg, Pore size distributions, pore coupling, and transverse relaxation spectra of porous rocks, Magn. Reson. Imag. 12 (2) (1994) 271–274.
[23] P.C. Chaves, A. Taborda, J.P. Marques, M.A. Reis, N to K Uranium PIXE spectra obtained at the high resolution high energy PIXE setup, Nucl. Instrum. Methods Phys. Res. B 318 (2014) 60–64.
[24] M.A. Reis, P.C. Chaves, A. Taborda, J.P. Marques, N.P. Barradas, CdTe and EDS HR-PIXE Ta L and M spectra induced by duoplasmatron generated proton and oxygen ion beams, Nucl. Instrum. Methods Phys. Res. B 417 (2018) 32–36.
[25] P.C. Chaves, M.A. Reis, H^+, O^{+2}, O^{+3} high resolution pixe spectra of Yb_2O_3, Nucl. Instrum. Methods Phys. Res. B 410 (2017) 193–199.
[26] S. Meiboom, D. Gill, Modified spin-echo method for measuring nuclear relaxation times, Rev. Sci. Instrum. 29 (1958) 688–691.
[27] M.A. Reis, S. Pessanha, P.C. Chaves, M.L. Carvalho, Reaching for copper pigments speciation with High Resolution Energy Dispersive PIXE. Nucl. Instrum. Methods Phys. Res. B, (in press), 2019.
[28] M. El Ouahabi, G. ChOne, D. Strivay, J. Vander Auwera, A. Hubert-Ferrari, Inter-technique comparison of PIXE and XRF for lake sediments, J. Anal. At. Spectrom. 883 (33) (2018) 883–892.
[29] Kristina Keating, Rosemary Knight, A laboratory study to determine the effect of iron oxides on proton NMR measurements, Geophysics 72 (2007) F27–F32.
[30] Kristina Keating, Rosemary Knight, A laboratory study of the effect of Fe(II)-bearing minerals on nuclear magnetic resonance (NMR) relaxation measurements, Geophysics 75 (2010) F71–F82.
[31] S. Limandri, J. Robledo, G. Tirao, Extracting chemical information from high-resolution Kβ X-ray emission spectroscopy, Spectrochim. Acta Part B 44 (2018) 29–37.
[32] P.C. Chaves, A. Taborda, N.P. Barradas, M.A. Reis, CdTe detector use for PIXE characterization of TbCoFe thin films, Nucl. Instrum. Methods Phys. Res. B 268 (2010) 2010–2014.